Improved slicing strategy for digital micromirror device-based three-dimensional lithography with a single scan

Shengzhou Huang, Mujun Li ✉, Lianguan Shen, Jinfeng Qiu, Youquan Zhou

Department of Precision Machinery and Precision Instrumentation, University of Science and Technology of China, Hefei 230026, Anhui, People's Republic of China
✉ *E-mail: lmn@ustc.edu.cn*

Published in Micro & Nano Letters; Received on 26th June 2016; Accepted on 11th October 2016

To improve the profile quality of three-dimensional microstructures, an improved method was proposed in real-time maskless lithography based on digital micromirror device. First, to calculate the spatial distribution of exposure dose for the target profile in design, the relations of the exposure dose and the development depth were investigated. Moreover, a suitable development time was obtained. Second, an improved slicing strategy based on equal-arc algorithm was proposed to reduce the profile error. Different from traditional equal-expose-dose method, this method generated slicing layers with equal arc-length instead of equal-exposure dose. Such an approach has advantages in obtaining a series of suitable section patterns adapting to the curvature variation of the design profile. Finally, an aspheric microlens array was fabricated with this method and the equal-exposure-dose method. Results showed that the resulting microstructure profile by their method was more consistent with the design profile with the same slicing numbers. Moreover, results also showed that the method used can obtain as good profile quality as that of the equal-exposure-dose method with only a half of slicing numbers. This indicated that the proposed method is feasible for achieving good profile quality with slicing efficiency improved remarkably.

1. Introduction: Three-dimensional (3D) microstructures have a wide variety of applications in the optics and photoelectric systems, microelectromechanical systems, and sensors [1, 2], because of superior performance, compact, easy to integrate etc. Several types of 3D photolithography techniques have been proposed including grey-scale mask lithography [3, 4], moving mask lithography [5], 3D diffuser lithography [6], multilayer lithography, and inclined lithography [7–9] etc. However, these techniques are quite complicated, high cost, long cycle, and require a physical mask, which is difficult to design and expensive to fabricate over a large area.

In recent years, maskless lithography technique based on a digital micromirror device (DMD) has become a promising approach, which is convenient to perform the 3D microstructures fabrication. Since this technique can use a virtual mask generated by computer instead of a physical mask, it avoids the associated costs of using a physical mask and improves the turnaround time. Moreover by this way, the mask pattern in the fabrication process can be changed continuously in real time. Typically, 3D microfabrication by the technique is performed either in a layer-by-layer fashion such as in microstereo-lithography [10, 11] or by the scanning method [12] in a manner similar to direct-writing imaging technique. Nevertheless, both of the two methods have the problem of misalignment error, lack of repeatability, and time consuming. To avoid the influence of these factors, a single scan method was developed recently, in which the fabrication process of 3D microstructure was finished by one-time scan. Generally, the maskless lithography technique fabricates a 3D microstructure by the multilayer slicing approach to obtain the approximately continuous profile. Slicing strategies such as equal-height scan applied in the 3D printing region and equal-exposure-dose scan strategy [13, 14] have been developed. However, the profile precision is mainly guaranteed by a large number of slicing layers and the efficiency of fabrication is limited.

In the equal-exposure-dose strategy, the profile quality is co-determined by the total exposure dose and the amount of slices. Hence, when the designed target profile is a curve with variant curvature, the method would not adapt to the change of curvature well, which will cause a big profile error with respect to the design profile. In this Letter, we present an improved slicing method using a single scan method [13, 14] based on maskless lithography technique. The new approach which we call equal-arc-mean slicing strategy was based on equal-arc slicing. The method could accommodate the change of curvature of the design profile very well and generate a series of suitable section pattern. This method could achieve as good profile accuracy as what achieved in the equal-exposure-dose method, while decreasing the slicing layers amounts efficiently. The experiment system and principles of the fabrication method will be demonstrated, and fabrication of an aspheric microlens array will also be discussed for evaluation of this method.

2. Prototype lithography system: The schematic diagram of DMD-based maskless lithography prototype system was designed as shown in Fig. 1. The system mainly contained four major parts: the uniform illumination system, the DMD system, the charge coupled device (CCD) focusing control system, and the projection system. The doublet lens in the system were used as the tube lens to correct the chromatic aberration, which helped to improve the imaging quality. The resolution of the system can reach ~2 µm.

2.1. Uniform illumination system: It included a high-pressure mercury lamp, liquid light guides, and an adjustable collimator. The mercury lamp (OmniCure™ S1500, EXFO Co., Canada) with output of 200 W was used as the ultraviolet source, which was filtered to emit light at a wavelength of 365 nm. Moreover, the liquid light guides and adjustable collimator (EXFO Co., Canada) played the role of making illumination uniform and light collimating, respectively.

2.2. DMD system: The DMD in our system consists of an array of 1024×768 micromirrors of which each size is 13.68×13.68 µm. Each micromirror can be tilted to the on or off state, in which the incident light is reflected toward the projection plane or to a light dump, respectively. The corresponding tilted angles are +12° and −12°. Each micromirror of DMD stands for a pixel of the binary images generated in real time by computer. The process of

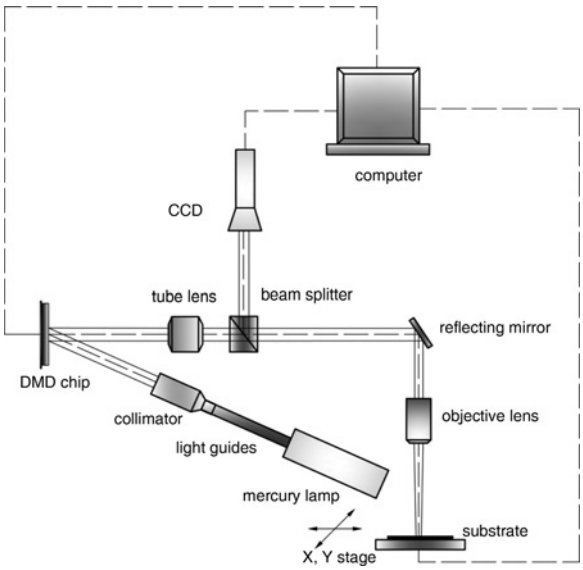

Fig. 1 *Schematic diagram of DMD-based maskless lithography prototype system*

generating digital masks was controlled in a graphical user interface which is realised by ourselves with the C/C++ programming.

2.3. CCD focusing control system: This function was realised by a beam splitter prism and a CCD image acquisition system, which would help focusing in projection.

2.4. Projection system: The system, which consisted an objective with numerical aperture of 0.13 (CFI Plan Flour ×4, Nikon Co., Japan), could project an image covering an area of ~2.65 × 1.99 mm, addressing 786,432 pixels, each of which was 2.44 μm in size. The focal depth and the working distance of the objective lens are 10.8 μm and 17.5 mm, respectively.

3. Equal-arc-mean method in 3D microstructure fabrication: On the basis of the maskless lithography system designed, we proposed the process as schematically illustrated in Fig. 2. First, the spatial distribution of the exposure dose was calculated for the target profile of a photo-resist structure designed to be fabricated. The calculations were according to the relationship of the exposure dose and the development depth with a suitable development time obtained by the Poor Man's dissolution rate monitor (DRM) approach [15, 16]. As shown in Fig. 2*a*, the curve $h(x, z)$ was the designed target profile, and the development depth of photo-resist was assumed to be a logarithmic function of exposure dose [17]. For a certain positive photo-resist, there exists the exposure threshold E_{th} and E_c, which are defined as the minimum exposure dose of triggering photo-resist reaction and

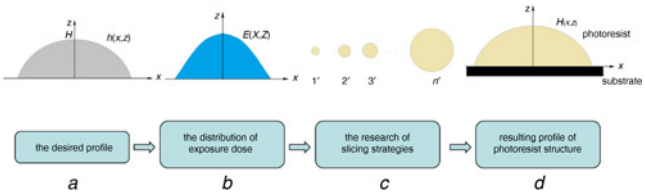

Fig. 2 *The schematic of the process for applying a single scan method*
a Design profile
b Distribution of exposure dose
c Research of slicing strategies
d Resulting profile

the required exposure dose that the photo-resist is completely removed from the substrate, respectively. The total height of the resulting profile was supposed to be H. The value of contrast, which is related to the photo-resist thickness, also has the contribution to the final target profile. Moreover, the value of contrast γ was defined as the linear slope of the contrast curve, as shown in (1) [17].

According to (1), the distribution of exposure dose $E(x, z)$ for

$$\gamma = \frac{1}{\ln E_c - \ln E_{th}} = \frac{h(x,\ z)}{H[\ln E(x,\ z) - \ln E_{th}]} \tag{1}$$

where $0 \le h(x,\ z) \le H$ and $E_{th} \le E(x,\ z) \le E_c$ the design profile can be deduced, as shown in (2)

$$E(x,\ z) = \exp\left(\frac{h(x,\ z)}{H\gamma} + \ln E_{th}\right) \tag{2}$$

After obtaining the distribution of exposure dose, the slicing strategies were investigated, which aimed to improve the profile quality and the fabrication efficiency. Generally, the equal-exposure-dose method is a common scanning strategy applied in the slicing process to restructure the design profile. The slicing process of this strategy is as follows: for n layers profile quantified, the exposure dose of each layer was E_c/n. Combined with the spatial distribution of exposure dose, the cross-section radius of every layer can be calculated. Then, the resulting profile could be restructured by the accumulation of exposure dose of each layer. In this method, the precision of the resulting profile is determined by the amount of slicing layers, which will greatly limit the processing efficiency.

Therefore, an improved strategy was proposed based on the equal-arc slicing. As shown in Fig. 3, assuming that the design profile with height H is divided into n segments, each of which has an equal arc-length of ΔL, as described in (3)

$$\cap h1 = \cap h2 = \cdots = \cap hn = \Delta L \tag{3}$$

Then according to the segmentation, in the equal-arc slicing scan method, the design profile could be sliced to n layers either with an inscribed step line as indicated by the dashed line, or with a circumscribed step line as indicated by the solid line, as shown in Fig. 3. Here different from the equal-arc slicing, to obtain a more accurate profile we adopted an equal-arc-mean scanning strategy, in which the circumscribed and inscribed layers are averaged. Thus, the corresponding radius of the ith layer r_i' can be expressed as (4)

$$r_i' = \frac{r_i + r_{i-1}}{2} \text{ for } r_1' = \frac{r_1}{2}, \quad i = 2,\ \ldots,\ n. \tag{4}$$

4. Analysis and discussion of experiments results: To evaluate the validity of the proposed method, an aspheric microlens array was studied as an example. The design profile equation of each aspheric microlens is shown in (5). The parameters of R and H

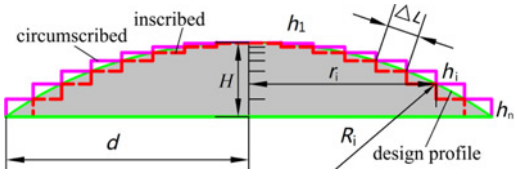

Fig. 3 *Schematic diagram of the equal-arc-mean scan*

doi: 10.1049/mnl.2016.0420

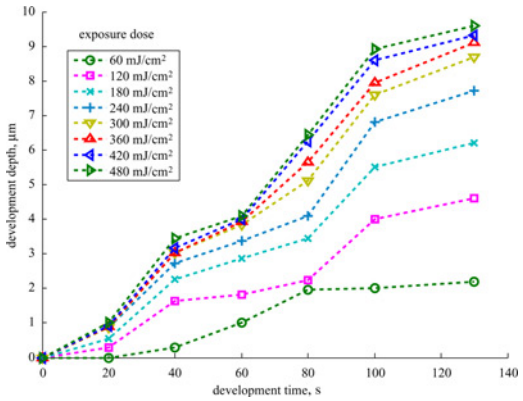

Fig. 4 *Experimental results of the development depth dependence on the development time for various exposure doses*

were set to 50 and 9 μm, respectively

$$\frac{x^2+y^2}{R^2}+\frac{z^2}{H^2}=1, \quad 0\le z\le H \tag{5}$$

Since the resulting profile was mainly co-determined by the exposure dose, the development time, and the development depth, to obtain a suitable development time for a total profile height, it was necessary to investigate the relations of these three factors. Fig. 4 showed the experimental results of the relation of the three factors by using the Poor Man's DRM approach. According to the analysis of the dissolution rate with a fixed development time could be obtained.

Obviously, it can be seen that the dissolution rate increased with increasing of the exposure dose. Moreover, for a certain exposure dose, the development depth was also increased with increasing of the development time. During the development process, the unexposed parts of photo-resist were also partially dissolved. Hence, for a required development depth, reducing the development time appropriately was very important to diminish the influence of photo-resist dissolution. In our study case, the total height H in (5) was set to 9 μm. According to the relation of exposure dose and development depth as shown in Fig. 5, for a 9 μm thick photo-resist film the required exposure dose was determined to be 360 mJ/cm^2. Then, according to the measured results in Fig. 4, it can be seen that the 130 s development time was a suitable time chosen to investigate the relationship between the exposure dose and development depth.

To obtain the exposure threshold and the contrast value, a fundamental experiment was performed on the silicon substrate. The basic conditions of the lithography process for AZ P4620 (Clariant Corporation) photo-resist were shown in Table 1. According to the measurement results, the relation of exposure dose and development depth was fitted to a curve as shown in Fig. 5. From this curve, the exposure threshold E_{th} and the contrast γ of the photo-resist were determined to be 35.8845 mJ/cm^2 and 0.4604, respectively. Then, the exposure dose distribution for the design profile can be calculated according to (2) as shown in Fig. 6.

Table 1 Basic lithography process conditions of AZ P4620

Lithography process	Process parameters
coating	2000 rpm, 9.5 μm thick
soft-bake	100°C, 6 min
exposure	365 nm, 10 mw/cm^2, 36 s
development	AZ 400 K: DI water = 1:4, 130 s
rinsing	DI water

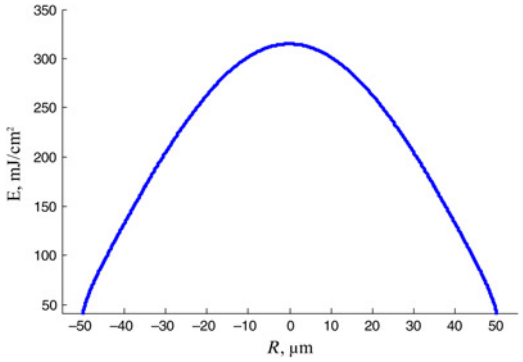

Fig. 6 *Distribution of exposure dose for the design profile*

Here, to compare the effect of different slicing strategies, and for the consideration of the proportional relationship between the slicing amounts and profile accuracy, the amounts of slicing layers were set to ten layers. The comparison diagram for different slicing strategies relative to the design profile was shown in Fig. 7. The profile measurements were performed with Bruker Stylus Profiler-DektakXT.

Fig. 8 also showed the scanning electron microscope (SEM) photographs of the microlens arrays with different strategies. From Fig. 7, it can be seen that with the equal-arc-mean strategy we could obtain a better profile compared with that of the equal-exposure-dose strategy. When the slicing amounts for the

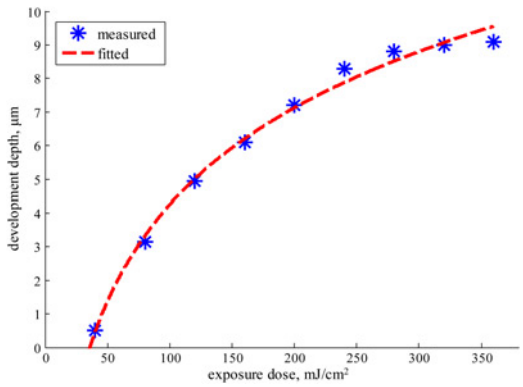

Fig. 5 *Relation of exposure dose and developed depth with a fixed development time*

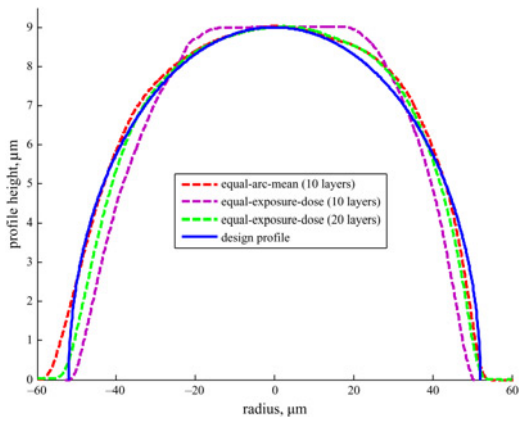

Fig. 7 *Comparison diagram for different slicing strategies relative to the design profile*

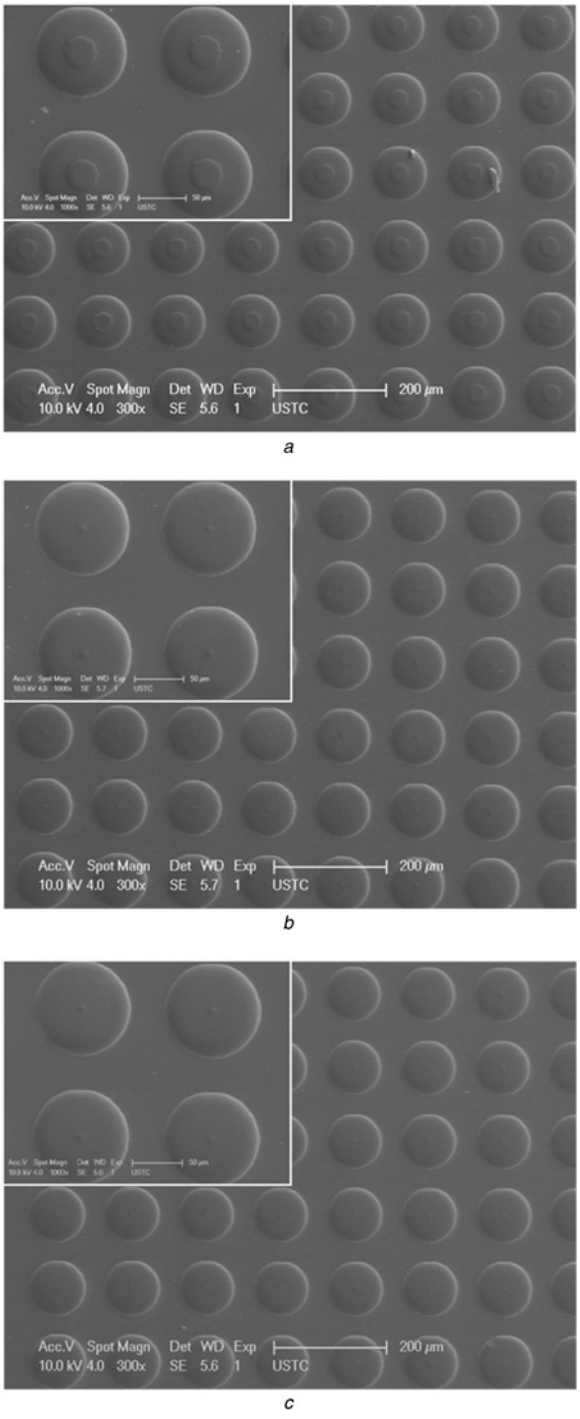

Fig. 8 *SEM photographs of fabricated microlens array*
a Equal-exposure-dose (ten layers)
b Equal-exposure-dose (20 layers)
c Equal-arc-mean (ten layers)

equal-exposure-dose were increased to 20 layers, the resulting profile was close to the one resulted in the equal-arc-mean strategy with only ten layers. This indicated that our slicing strategy could improve the processing efficiency significantly, without more subdivision of slicing layers.

5. Conclusion: A prototype system based on DMD maskless lithography was designed and implemented. An improved slicing strategy based on the equal-arc slicing was proposed in microstructure fabrication with a single scan. It can be adaptable with the contour curvature adaptive change, and obtain a series of suitable cross-section graphics. Compared with the traditional equal-exposure-dose slicing strategy, this method demonstrated the capability of achieving high-quality profile with the fabrication efficiency improved remarkably. As this kind of fabrication method is real time, maskless, cost effective, and with no alignment error, it is expected to have a broad application prospect in fabrication of microoptics elements with variable curvature or complex shape. Future work will involve the investigations to compensate profile error and smooth the contour surface, combining the proposed method with the thermal reflow technique.

6. Acknowledgments: This work was supported by funding from the Chinese National Natural Science Foundation (grant no. 51475442), the Fundamental Research Funds for the Central Universities, and partially carried out at the University of Science and Technology of China Center for Micro and Nanoscale Research and Fabrication.

7 References

[1] Yoon Y.-K., Park J.-W., Allen M.G.: 'Polymer-core conductor approaches for RF MEMS', *J. Microelectromech. Syst.*, 2005, **14**, (5), pp. 886–894
[2] Perdigones F.A., Moreno J.M., Luque A., *ET AL.*: 'Characterisation of the fabrication process of freestanding Su-8 microstructures integrated in printing circuit board in microelectromechanical systems', *IET Micro Nano Lett.*, 2010, **5**, (1), pp. 7–13
[3] Waits C., Morgan B., Kastantin M., *ET AL.*: 'Microfabrication of 3D silicon MEMS structures using gray-scale lithography and deep reactive ion etching', *Sens. Actuators A*, 2005, **119**, (1), pp. 245–253
[4] Zhang J., Guo C., Wang Y., *ET AL.*: 'Micro-optical elements fabricated by metal-transparent-metallic-oxides grayscale photomasks', *Appl. Opt.*, 2012, **51**, (27), pp. 6606–6611
[5] Hirai Y., Inamoto Y., Sugano K., *ET AL.*: 'Moving mask UV lithography for three-dimensional structuring', *J. Micromech. Microeng.*, 2006, **17**, (2), p. 199
[6] Lee H.S., Yoon J.-B.: 'A simple and effective lift-off with positive photoresist', *J. Micromech. Microeng.*, 2005, **15**, (11), p. 2136
[7] Mata A., Fleischman A.J., Roy S.: 'Fabrication of multi-layer Su-8 microstructures', *J. Micromech. Microeng.*, 2006, **16**, (2), p. 276
[8] Devaraju N.S.G.K., Unger M.A.: 'Pressure driven digital logic in PDMS based microfluidic devices fabricated by multilayer soft lithography', *Lab. Chip*, 2012, **12**, (22), pp. 4809–4815
[9] Jiang G., Baig S., Wang M.R.: 'Prism-assisted inclined UV lithography for 3D microstructure fabrication', *J. Micromech. Microeng.*, 2012, **22**, (8), p. 085022
[10] Choi J.-W., Irwin M.D., Wicker R.B.: 'DMD-based 3D micromanufacturing'. Proc. Int. Conf. on Emerging Digital Micromirror Device Based Systems and Applications, San Francisco, CA, 23 January 2010, vol. 7596, p. 75960H
[11] Choi J.-W., Wicker R.B., Cho S.-H., *ET AL.*: 'Cure depth control for complex 3D microstructure fabrication in dynamic mask projection microstereolithography', *Rapid Prototyping J.*, 2009, **15**, (1), pp. 59–70
[12] Totsu K., Fujishiro K., Tanaka S., *ET AL.*: 'Fabrication of three-dimensional microstructure using maskless gray-scale lithography', *Sens. Actuators A*, 2006, **130**, pp. 387–392
[13] Zhong K., Gao Y., Li F., *ET AL.*: 'Fabrication of continuous relief micro-optic elements using real-time maskless lithography technique based on DMD', *Opt. Laser Technol.*, 2014, **56**, pp. 367–371
[14] Hur J.-G.: 'Maskless fabrication of three-dimensional microstructures with high isotropic resolution: practical and theoretical considerations', *Appl. Opt.*, 2011, **50**, (16), pp. 2383–2390
[15] Thornton S.H., Mack C.A.: 'Lithography model tuning: matching simulation to experiment'. Proc. Int. Conf. on Microlithography, Santa Clara, CA, 10 March 1996, vol. 2726, pp. 223–235
[16] Hirai Y., Sugano K., Tsuchiya T., *ET AL.*: 'A three-dimensional microstructuring technique exploiting the positive photoresist property', *J. Micromech. Microeng.*, 2010, **20**, (6), p. 065005
[17] Ueno T.: 'Microlithography: science and technology' (Marcel Dekker, US, 1998)

doi: 10.1049/mnl.2016.0420